Original Research Paper Physics

Thermoelectric Properties of Bismuth Telluride Nanocomposites Reinforced with Graphene

Ravindra Kumar Department of Physics, M.M.H.College Ghaziabad-201001, India, * Corresponding author

ABSTRACT

The thermoelectric properties of nanostructured bismuth telluride and its nanocomposites with 0.3 wt% graphene are reported in this communication. Nanocomposites of bismuth telluride were synthesized by using high energy ball-milling technique followed by pressing at 4 kN/m2 and sintering at 573K temperature in vacuum. XRD was used for crystallographic investigations, and phase determination. Transmission electron microscopy (TEM) and scanning electron microscopy (SEM) were used to analyze microstructure, particles shape, size and surface morphology of the synthesized materials. Thermoelectric parameters such as Seebeck coefficient, electrical conductivity, thermal diffusivity, specific heat and figure of merit and of the samples were determined. Nanocomposite of bismuth telluride reinforced with 0.3% by wt graphene has been synthesized and an improvement in its figure of merit was observed which was due to significant decrease in its thermal conductivity, due to increase phonon scattering by graphene.

KEYWORDS : Thermoelectric properties, nanocomposites, figure of merit

INTRODUCTION

It is known that of all the primary energy we harness and use, only 30% is translated into useful work. A staggering 70% is wasted as dissipated heat during energy conversion, transportation and storage [1]. This huge loss is itself a source of recyclable energy. If this waste heat could be harnessed employing thermoelectric devices, it could lead to additional available green energy resources [2-3]. However, the present use of TE devices is limited by their low efficiencies. To achieve the goal of high-efficiency energy conversion the current traditional TE materials are not satisfactory, having new generation TE materials will have to be developed to bring about substantial impacts [4].

Thermoelectric devices based on bismuth telluride are widely used in the fabrication of thermal sensors, laser diodes, thermoelectric refrigeration for cooling and power generation [5-6]. Efficiency of the thermoelectric material depends on its figure of merit $ZT = S^2\sigma T/ k$ [7]. Where, ZT= figure of merit, α = Seebeck's coefficient or thermoelectric power, σ = electrical conductivity, T=Temperature and k= thermal conductivity. In order to increase the thermoelectric efficiency of the material we need to improve the figure of merit. With the advent of sophisticated materials processing techniques, novel nanostructures with enhanced figure-of-merit (ZT) have been realized in wide variety of materials, such as tellurides, silicides, skutterudites, and others [8]. Although high ZT values were reported in superlattice structures and nano-wires/rods, it has proven difficult to use them in large-scale energy-conversion applications because of limitations in both heat transfer and cost [9-10]. Bi_2Te_3 is an excellent thermoelectric material which has been widely used for refrigeration applications at room temperature. However, the ZT needs to be further increased in order to enhance the efficiency and the performance. The figure of merit can be increased by increasing electrical conductivity, improving thermoelectric power and reducing thermal conductivity. Heat in solids is conducted by various carriers: electrons, lattice wave (or phonons), magnetic excitations and in some cases electromagnetic radiations [11-12]. The presence of nanostructures, which increase the grain boundary concentration in the materials, can enhance phonon scattering at grain boundaries, resulting in marked decrease in thermal conductivity [13]. However, due to the high density of grain boundaries, electrons are also scattered efficiently, leading to a concurrent decrease in electrical conductivity. We need to suppress phonon conductivity rather than reducing thermal conductivity due to electrons, as the flow of electrons due to thermal potential aids the development of thermoelectric EMF [14]. One of the best methods to reduce phonon conductivity is by increasing the number of interfaces encountered by the phonons in the material. Bulk material made by compressing the nanoparticle will offer increased interface in the path of the phonons. Addition of foreign nanostructure materials also increases the interface [15-17].

In the present work we have used graphene as a reinforced material to make Bi_2Te_3 nanocomposites by using ball milling process followed by consolidation sintering. The advantage of this planner material is that, one can easily change its electronic properties by introducing tunable gap in the sample or changing the number of graphene planes [18-19]. It has a very high electrical conductivity at room temperature due to its very large mobility [20]. However, the ability of graphene to conduct heat is an order of magnitude higher than that of copper. Therefore, it is necessary to reduce its thermal conductance for thermoelectric application. The high thermal conductance of graphene is mostly due to the lattice contribution, whereas the electronic contribution to the thermal conduction can be ignored. Therefore, by proper engineering of phonon transport properties it is possible to reduce the total thermal conductance without significant reduction of the electrical conductance and the power factor [21]. If a small quantity of graphene is embedded into the Bi_2Te_3 matrix, it is expected that, Bi_2Te_3+0.3% graphene nanocomposite has large number of grain boundary may exert some detrimental effect on the thermal conductivity while simultaneously maintaining the high electrical conductivity.

EXPERIMENTAL

2.1 *Synthesis of Bi_2Te_3/ Bi_2Te_3+0.3% graphene Nanocomposites:*

Bi_2Te_3 bulk compound was synthesized by using vertical directional solidification (VDS) method. A small piece was taken from the as synthesized Bi_2Te_3 bulk compound ingot and ground manually in the astle to form powder. This manually grinds Bi_2Te_3 powder and its mixture with 0.3% by wt pure graphene was further ball milled (BM) at the rate of 200 rpm for 4 hrs in Ar atmosphere to obtain fine powders. Zirconia balls were used for milling at a ball to powder weight ratio of 10:1. Petroleum ether was added in mixture to prevent agglomeration of fine particles induced due to heating effect during ball milling process. Mechanical alloying is a proven, low cost technique for synthesis of thermoelectric materials. After ball milling these powders were compressed under the pressure of 4 kN/m^2 for 2 min to form pellets, which were sintered at 573K for 2 hrs in vacuum of the order of 10^{-3} torr.

2.2 *Characterization of Bi_2Te_3/ Bi_2Te_3+0.3% graphene Nanocomposites***:**

Phase and structures of the synthesized composites were investigated by XRD technique using CuK_α line radiation. Surface morphology and elemental analysis were performed by using scanning electron microscopy (SEM, make Leo model EVOMA10) and energy dispersive spectroscope (EDS: oxford ISIS 300) attached with SEM. Grain size, shape and microstructures were investigated by using high resolution transmission electron microscope (HRTEM) make FEI, model Tecnai G2 F30 STWIN operated at 300 kV. Thermal diffusivity Seebeck coefficient, and electrical conductivity were determined by using Laser Flash Technique (Linseis, LFA 1000 and Ulvac, ZEM 3). Specific heat of the composite was measured by using differential scanning calorimeter (Mettler Toledo, DSC842). Thermal conductivity 'K' was calculated using the formula $k=d\,\rho\,C_p$ where ρ is the sample density, d is thermal diffusivity and C_p is specific heat. Density of the samples was deter-

mined by using Archimedes kit.

RESULT AND DISCUSSION

Powder XRD measurements were carried out by using Cu k_α line radiation with wavelength 1.54059Å on 4 hrs ball mill Bi_2Te_3 and its composite reinforced with 0.3% graphene respectively. The data was recorded in 2θ range of 10–80 degree with step size of 0.01°. A typical XRD pattern of the 4 hrs ball milled Bi_2Te_3 powder and its composite with 0.3% graphene is shown in Fig.1. The XRD pattern shown in Fig.1 curve (a) consists of all possible reflection of Bi_2Te_3 with sharp peaks which indicates the formations of single phase and polycrystalline nature of Bi_2Te_3 nanocomposites having hexagonal structure and ($R\bar{3}m$) space group. The results were found to be in good agreement with standard values of JCPDS file No. (82-0358) of Bi_2Te_3 having rhombohedral structure. Fig.1 curve (b) represents the XRD pattern of ball milled Bi_2Te_3 nano composite reinforced with graphene (Bi_2Te_3+0.3% graphene). Thorough analysis of the XRD pattern does not shows any reflection of graphene. This may be due to the fact that we have used only 0.3% graphene in Bi_2Te_3 nanocomposite matrix which is much lower in quantity to be detected in the XRD measurement. XRD pattern of graphene has been shown in Fig.2 indicating the reflection peaks corresponding to (111), (010) and (222) plane having rhombohedral structure which are in good agreement with JCPDS file no. 75-2078. The strain (η) developed in the composite during synthesis process has been evaluated using the Hall-Williamson relation: $\beta\cos\theta = \kappa\lambda/\tau + \eta\sin\theta$, where, β, θ, κ, λ, τ, and η are FWHM (full width at half maximum) of the diffraction peak in radians, Bragg diffraction angle of the peak (half of the peak position on the 2θ-axis), Scherrer constant, wavelength of X-rays, crystallite size, and strain distribution within the materials respectively. Slope of linear fit of the data points directly gives the value of η. The values of η for Bi_2Te_3 bulk compound and its composite reinforce with 0.3% graphene are found to be 0.28 and 0.30 respectively. X-ray diffraction peaks are broadened by small grain-size and by lattice distortions caused by lattice defects.

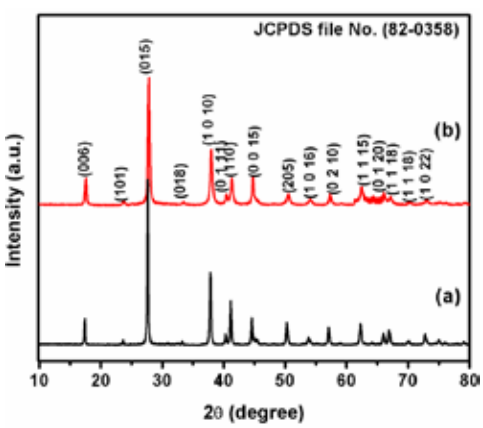

Figure 1 curve (a) XRD pattern of Bismuth Telluride ball milled for 4 hrs and curve (b) XRD pattern of Bi_2Te_3+0.3% graphene ball milled for 4 hrs.

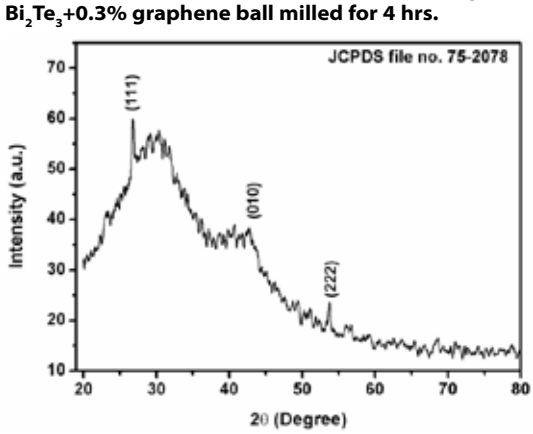

Figure 2. XRD pattern of grapheme

Surface morphology of Bi_2Te_3+0.3% graphene pellets after sintered at 573K temperature was investigated by using scanning electron microscope (SEM). Fig.3 (a) shows SEM image of Bi_2Te_3+0.3% graphene pellet after sintered at 573K and recorded at low magnification revealing morphology of top surface. SEM micrograph shows the flattened surface due to applied pressure of 4 kN/m^2. Further magnified image of the top surface of the pellet revealed the presence of micro pits (Fig.3b). A small broken piece was also taken from the pellets for further investigation under SEM. Fig.3(c) and 3(d) shows the SEM images of the broken area of the pallets revealing the presence of micro and nano pores. Fig. 3(d) Shows morphology and arrangement of Bi_2Te_3 particles having platy and granular shape particle of size varying between 150 nm to 1.5μm for 4 hrs ball mill and 10:1 ball to materials weight ratio.

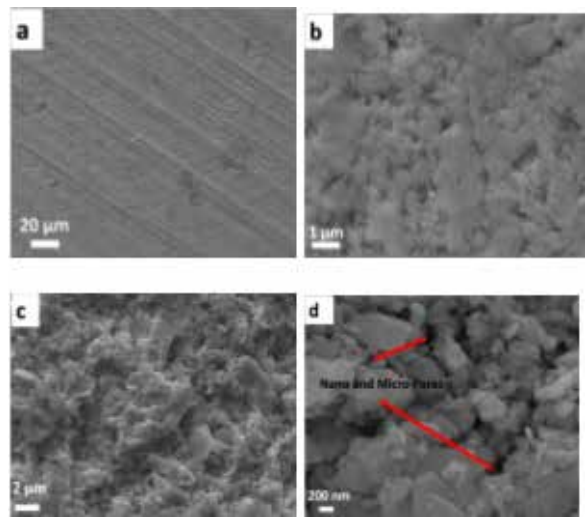

Figure 3(a) SEM image of top surface of pellet, (b) further magnified image of same area, (c) image of broken area, (d) further magnified image of broken area.

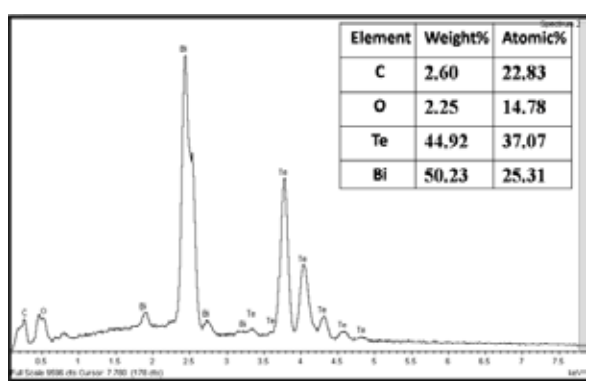

Figure 4 EDS spectrum of Bi_2Te_3+0.3% graphene nanocomposite

As synthesized graphene based Bi_2Te_3 nano composites were examined for elemental analysis and stoichiometry by energy dispersive spectrometer (EDS: oxford ISIS 300) attached to scanning electron microscope (SEM: Leo EVOMA10). From the EDS spectra as shown in Fig.3 it is observed that stoichiometry of Bi and Te in Bi_2Te_3+0.3% graphene is nearly maintained with presence of graphene (carbon). The presence of oxygen as observed in the EDS spectra of the composite may be due to trapped oxygen in the micro and nano pores in the composite sintered in the vacuum of the order of $5x10^{-3}$ torr.

Microstructural features associated with Bi_2Te_3+0.3% graphene nanocomposite was examined under high resolution transmission electron microscope (HRTEM operated at accelerating voltage of 300KV. Fig.4(a) shows TEM image of Bi_2Te_3 nanocomposite revealing sheet/layered like structure of Bi_2Te_3 nano particles consisting of the particle size between 300nm to 1 um. Presences of graphene sheets are clear-

ly visible in the TEM micrograph as marked in the image. Selected area electron diffraction patterns (SAEDP) of the corresponding area revealing ring pattern shows polycrystalline nature of the material. Detailed analysis of SAEDP suggests the growth along (1 0 10), (006) and (015) oriented planes of Bi_2Te_3 having rhombohedral structure. The results of electron diffraction pattern of Bi_2Te_3 are in good agreement with the JCPDS file No. (82-0358)

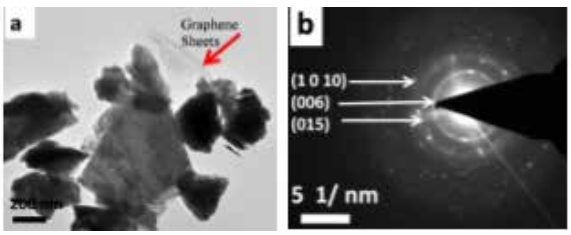

Figure 5(a) TEM image of Bi_2Te_3 nanocomposite shows the attachment of Bi_2Te_3 particle with graphene sheet. (b) represents the corresponding SAEDP of Bi_2Te_3+0.3% graphene nanocomposites.

The thermoelectric parameters such as thermal diffusivity, Seebeck coefficient and electrical conductivity of the nanocomposite of Bi_2Te_3 and Bi_2Te_3+0.3% graphene nanocomposites were determined by using Laser Flash Technique (Linseis, LFA 1000 and Ulvac, ZEM 3) and are shown in Fig.6. Fig.6(a) shows the plot between electrical conductivity and temperature for nanocomposites of Bi_2Te_3 and Bi_2Te_3+0.3% graphene. It is observed that electrical conductivity increases with temperature for the both the composites showing the semiconducting behavior of these nanocomposites. It is important to mention here that the electrical conductivity for Bi_2Te_3+0.3% graphene composite was found to be increased by 4.4% as compared with the nanocomposites of Bi_2Te_3. However the Seebeck coefficient of Bi_2Te_3+0.3% graphene nanocomposites was found to be decreased as compared to nanocomposites of Bi_2Te_3 as shown in (Fig.6b). Fig.6(c) represents the change in thermal conductivity as a function of temperature for nanocomposites of Bi_2Te_3 and Bi_2Te_3+0.3% graphene. It is observed that the thermal conductivity of Bi_2Te_3+0.3% graphene nanocomposites has lower value than that of nanocomposite of Bi_2Te_3. Decrease in thermal conductivities of Bi_2Te_3+0.3% graphene nanocomposites may be due to the fact that addition of graphene have created more interfaces resulting more phonon scattering at interfaces of the grain boundaries. Carriers of heat in solids are electrons and lattice waves, leading to an overall thermal conductivity $k = k_{el} + k_{ph}$, where k_{el} is the electronics components and k_{ph} the lattice components. The carrier-related thermal conductivity k_{el} can be calculated from the electrical resistivity (ρ) according to the Wiedemann–Franz law: $k_{el} = LT/\rho$ [22], where L is the Lorentz constant and k_{el} and k_{ph} behave differently as function of temperature. For nano bulk Bi_2Te_3 and Bi_2Te_3+0.3% graphene nanocomposites k_{ph} forms appreciable components at room temperature. With the addition of graphene, k_{el}, according to the Wiedemann–Franz law and k_{ph}, is according to the phonon–grain boundary scattering decrease. This indicates that the lattice thermal conductivity has been efficiently restrained by the nanostructure, which enhances phonon–grain boundary scattering and results in a remarkable decrease in thermal conductivity, which results in improvement in the figure of merit of Bi_2Te_3+0.3%

graphene nanocomposites obtained in this work.

The maximum dimensionless figure of merit of the Bi_2Te_3+0.3% graphene nanocomposites is found to be 0.48 at 327K temperature, which is higher than the nanostructured Bi_2Te_3 (ZT=0.34) at the same temperature as depicted from Fig.6d. For further improvement in the thermoelectric efficiency of the Bi_2Te_3 based nanocomposites, efforts are being made by employing various process conditions. Thermoelectric parameters as observed during the study have been summarized in table 1. From the results summarized in the table, it is clearly evident that with reinforcement graphene in the nano structured Bi_2Te_3 an increase in ZT has been observed.

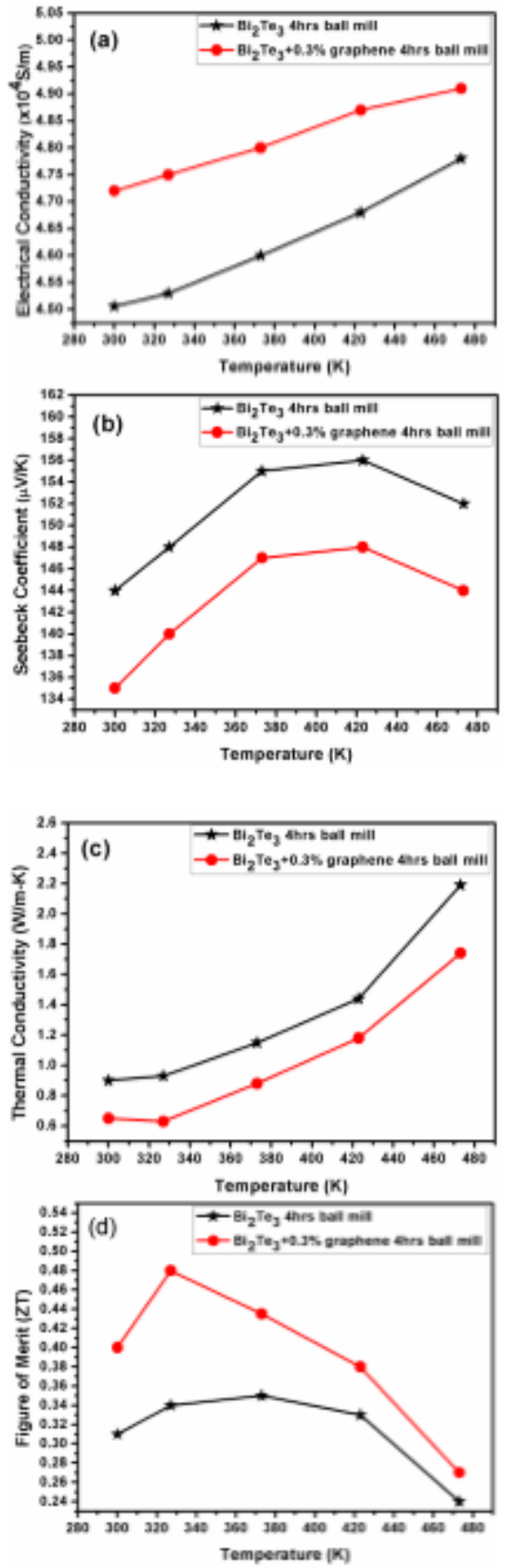

Figure 6 Temperature dependence of thermoelectric properties of 573K sintered n-type Bi_2Te_3 nanostructured alloys and Bi_2Te_3+0.3% graphene (a) electrical conductivity, (b) Seebeck coefficient (c) thermal conductivity (d) calculated ZT data.

Table 1. ZT values of ball milled and vacuum sintered nanostructured Bi_2Te_3 and its composite with 0.3 wt% graphene .

Sample	Electrical Conductivity (S/m)	**S.C. (μV/K)**	Thermal conductivity (W/m-K)	ZT
Bi_2Te_3	$4.53x10^4$	-148	0.93	0.34
Bi_2Te_3+0.3%graphene	$4.75x10^4$	-140	0.63	0.48

CONCLUSIONS

Nanostructured Bi_2Te_3 and its graphene reinforced nanocomposite have been synthesized by ball milling process under Ar atmosphere and were pelletized under the pressure of 4 kN/m^2 for 2 min. These pellets were sintered at 573K for 2 hrs in vacuum of the order of 10^{-3} torr. A noticeable variation in the thermoelectric parameters such as thermal conductivity, Seebeck coefficient and the calculated figure of merit ZT of graphene reinforced nanocomposite (Bi_2Te_3+0.3% graphene) have been observed. This study demonstrates that the figure of merit of Bi_2Te_3 nanocomposite is found to enhanced by incorporating graphene and it is expected that it would be a promising thermoelectric material for commercial applications. Effort are being made in order to achieve further higher ZT value by optimising the high energy ball milling process parameter followed by spark plasma sintering of Bi_2Te_3 nanocomposite reinforced with varying concentration of graphene.

REFERENCES:

[1] Fan S, Zhao J, Guo J, Yan Q, Ma J, Hng HH. p-type $Bi_{0.4}Sb_{1.6}Te_3$ nanocomposites with enhanced figure of merit. Appl Phy Lett 2010;96:182104-07

[2] Kim KT, Choi SY, Shin E H, Moon KS, Koo HY, Lee GG , Ha GH. The influence of CNTs on the thermoelectric properties of a CNT/Bi_2Te_3 composite. CARBON 2013; 52:541-549

[3] DiSalvo FJ.Thermoelectric cooling and power generation. Sci1999;285:703-706

[4] Li X, Ren H, Luo Y. Electronic structure of bismuth telluride quasi- two-dimensional crystal: A first principles study. Appl Phy Lett 2011;98: 083113-16

[5] Pundir SK, Singh S, Srivastava AK, Dalai MK, Kumar R. Influence of processing conditions on nanostructure Bi_2Te_3 thin films for their structural, electrical, and thermoelectric performance. Adv Sci Eng and Med. 2013;5:436-442

[6] Ma Y, Hao Q. Poudel B, Lan Y, Yu B, Wang D. Enhanced Thermoelectric Figure-of-Merit in p-Type Nanostructured Bismuth Antimony Tellurium Alloys Made from Elemental Chunks. Nano Lett. 2008;8:2580-2584

[7] Takashiri M, Tanaka S, Hagino H, Miyazaki K. Combined effect of nanoscale grain size and porosity on lattice thermal conductivity of bismuth-telluride-based bulk alloys. J Appl Phys 2012;112:084315-8

[8] Fan XA, Yang JY, Xie Z, Li K, Zhu W, Duan XK, Xiao CJ, Zhang QQ. Bi_2Te_3 hexagonal nanoplates and thermoelectric properties of n-type Bi2Te3 nanocomposites. J Phys D: Appl Phys 2007;40:5975–5979

[9] Poudel B, Hao Q, Ma Y, Lan Y, Minnich A, Yu B, Yan X, Wang D, Muto A, Vashaee D, Chen X, Liu J, Dresselhaus MS, Chen G, Ren Z. High-Thermoelectric Performance of Nanostructured Bismuth Antimony Telluride Bulk Alloys. Sci 2008;320: 634-638

[10] Snyder GJ, Toberer ES. Complex thermoelectric materials. Nat Mater 2008;7:105-114

[11] Li D, Sun RR, Qin XY. Improving thermoelectric properties of p-type Bi_2Te_3-based alloys by spark plasma sintering. Prog Nat Sci: Mater Inter 2011;21:336-340

[12] Gothard NW, Tritt TM, Spowart JE. Figure of merit enhancement in bismuth telluride alloys via fullerene assisted microstructural refinement. J Appl Phys 2011;110: 023706-6

[13] Zhou L, Zhang X, Zhao X, Sun C, Niu Q. Synthesis and characterization of carbon nanotube supported Bi_2Te_3 nanocrystals. J Alloy Compd 2010;502: 329-332

[14] Souza SM, Trichês DM, Poffo CM, Lima DJC, Grandi TA, Biasi DRS. Structural, thermal, optical, and photoacoustic study of nanocrystalline Bi_2Te_3 produced by mechanical alloying. J Appl Phys 2011;109:013512-8

[15] Poon SJ, Limtragool K. Nanostructure model of thermal conductivity for high thermoelectric performance. J Appl Phys 2011;110:114306-7

[16] Zhao LD, Zhang BP, Li JF, Zhang HL, Liu WS. Enhanced thermoelectric and mechanical properties in textured n-type Bi_2Te_3 prepared by spark plasma sintering. Solid State Sci 2008;10:651-658

[17] Li Z, Zhao GL, Zhang P, Guo S, Tang J.Thermoelectric Performance of Micro/Nano-Structured Bismuth-Antimony-Telluride Bulk from Low Cost Mechanical Alloying. Mater Sci Appl 2012;3:833-837

[18] Rabiu M, Y S. Mensah, S S, Abukari. General Scattering Mechanism and Transport in Graphene. Graphene 2013;2:49-54

[19] Li AH, Shahbazi M, Zhou SH, Wang GX, Zhang C, Jood P, Peleckis G, Dua Y, Cheng ZX, Wang XL, Kuo YK. Electronic structure and thermoelectric properties of Bi_2Te_3 crystals and graphene-doped Bi_2Te_3 .Thin Solid Films 2010;518:57-60

[20] Dragoman D, Dragoman M. Giant thermoelectric effect in graphene. Appl Phys Lett 2007;91:203116-3

[21] Karamitaheri H, Pourfath M, Pazoki M, Faez R, Kosinad H. Graphene-Based Antidots for Thermoelectric Applications. J Electrochem Soc 2011;158: 213-216

[22] Takashiri M, Miyazaki K, Tanaka S, Kurosaki J, Nagai D, Tsukamoto H. Effect of grain size on thermoelectric properties of n-type nanocrystalline bismuth-telluride based thin films. J Appl Phys 2008;104:084302-6.